Arabian Journal of Chemistry 16 (2023) 105313

Contents lists available at ScienceDirect

Arabian Journal of Chemistry

journal homepage: www.sciencedirect.com

Original article

Synthesis of biochar modified with 12-tungstophosphoric acid for the selective conversion of isoeugenol to vanillin

Ana Alice Farias da Costa [a,*], Alex de Nazaré de Oliveira [b], Rutiléia de Jesus Paiva [c], Luiza Helena de Oliveira Pires [a,d], Eloísa Helena de Aguiar Andrade [a,e], Patrícia Teresa Souza da Luz [f], Renata Coelho Rodrigues Noronha [g], Geraldo Narciso da Rocha Filho [a], Carlos Emmerson Ferreira da Costa [a], Sameh M. Osman [h], Rafael Luque [i,j], Luís Adriano Santos do Nascimento [a,c,*]

[a] Graduation Program in Chemistry, Federal University of Pará, Augusto Corrêa Street, Guamá 66075-110, PA, Brazil
[b] Universidade Federal do Amapá Campus Marco Zero do Ecuador, Rodovia Josmar Chaves Pinto Km 02, Jardim Marco Zero, Macapá 68903-419, AP, Brazil
[c] Graduation Program in Biotechnology, Federal University of Pará, Augusto Corrêa Street, Guamá 66075-110, PA, Brazil
[d] High School of Application, Universidade Federal do Pará, Belém, Pará CEP 66095 780, Brazil
[e] Adolpho Ducke Laboratory, Botany Coordinating, MuseuParaense Emílio Goeldi, Perimetral Avenue, Terra Firme, Belém, PA 66077-830, Brazil
[f] Federal Institute of Education, Science and Technology of Pará, Campus Belém, Avenue Almirante Barroso, Marco, Belém, PA 66093-020, Brazil
[g] Laboratory of Genetics and Cellular Biology - GENBIOCEL, Center for Advanced Biodiversity Studies, Institute of Biological Sciences, Federal University of Pará, Augusto Corrêa Street, Guamá 66075-110, PA, Brazil
[h] Department of Chemistry, College of Science, King Saud University, P.O. Box 2455, Riyadh 11451, Saudi Arabia
[i] Peoples Friendship University of Russia (RUDN University), 6 Miklukho Maklaya str., 117198 Moscow, Russian Federation
[j] Universidad ECOTEC, Km 13.5 Samborondón, Samborondón EC0922302, Ecuador

ARTICLE INFO

Article history:
Received 21 April 2023
Accepted 25 September 2023
Available online 29 September 2023

Keywords:
Waste valorization
Biochar
Heterogeneous catalysis
Isoeugenol oxidation
Vanillin
Amazon

ABSTRACT

A heterogeneous acid catalyst was synthesized by anchoring 12–tungstophosphoric acid (HPW) onto biochar derived from Brazil nut shells (*Bertholletia excelsa*). This catalyst was used for the synthesis of vanillin from isoeugenol, employing hydrogen peroxide in acetonitrile solvent. The HPW-functionalized biocatalyst was prepared using a sonication method, which avoids the need for toxic and corrosive solvents, effectively incorporating tungsten at a mass proportion of 25%. Characterization of the catalysts utilized various techniques, including X-ray diffraction, Fourier-transform infrared spectroscopy, scanning electron microscopy with energy-dispersive X-ray spectroscopy, and ultraviolet–visible spectroscopy. 30HPW/CC(200–2) exhibited high selectivity for vanillin (55%) with a significant conversion rate (69%). Over four cycles, selectivity and conversion remained consistently above 56% and 45%, respectively. The results presented in this study have the potential to promote a more sustainable vanillin production process, a valuable additive in the food and perfume industries, renowned for its high economic value.

1. Introduction

Vanillin is a widely employed flavoring agent utilized across multiple industries, including medicine, pharmaceuticals, food, beverages, and perfumery, for the purpose of masking undesirable odors or flavors. It finds common application in the manufacturing of ice cream, confectionery items, sweets, chocolates, and various other products. Notably, despite an annual demand of 12,000 tons, the production from natural sources only yields 1800 tons (Martău et al., 2021).

Vanillin can be prepared from eugenol (4-allyl-2-methoxyphenol) or isoeugenol [2-methoxy-4-(prop-1-en-1-yl) phenol] (Adilina et al., 2012). One approach to produce vanillin involves the catalytic oxidation of isoeugenol using hydrogen peroxide. However, this process usually necessitates the use of the costly and hazardous catalyst, methyltrioxorhenium (Gusevskaya et al., 2012). Hence, there is a need for alternative catalysts.

Molybdenum and tungsten oxides have shown promise as catalysts for the production of a wide range of fine chemicals due to

* Corresponding authors.
E-mail addresses: analilice@hotmail.com (A.A.F. da Costa), adriansantos@ufpa.br (Luís Adriano Santos do Nascimento).
Peer review under responsibility of King Saud University.

Production and hosting by Elsevier

https://doi.org/10.1016/j.arabjc.2023.105313
1878-5352/

their acidic properties (Ma and Dai, 2011). In certain instances, these catalytic species are supported by activated carbons (Petit et al. 2009; Alcañiz-Monge et al., 2013).

In recent years, the use of biomass-derived catalysts in chemical transformation processes has seen a substantial rise. This trend is attributed to the advantages it offers, including reduced energy consumption, streamlined operations, improved economics, and enhanced environmental sustainability (Lokman et al., 2016; Tamborini et al., 2019), As a result, a large proportion of residual biomass that would have otherwise been left to naturally decompose is now being utilized for the production of alternative sustainable catalysts (Araujo et al., 2019; Bastos et al., 2020; Corrêa et al., 2020; Costa et al., 2022; Mares et al., 2020).

Recently, several studies have investigated the use of natural plant residues from the Amazon rainforest for the production of activated carbon (Almeida et al., 2021; Mendonça et al., 2019; Queiroz et al., 2020; Reis et al., 2019). The aim of these studies is to develop catalysts based on residual biomass that can serve as adsorbents (Freitas et al., 2019; Rahman et al., 2019; Spagnoli et al., 2017), catalysts (Mares et al., 2020; Mendonça et al., 2019) and catalytic supports (Almeida et al., 2021). These efforts are justified not only by the recycling aspects of waste but also by the advantages of utilizing a renewable source, thereby mitigating significant adverse environmental impacts.

Most waste and biomass feedstocks generally lack intrinsic value. Nevertheless, pyrolysis is a commonly employed process to derive products such as biofuels and biochar, which possess a wide range of applications including their use in heterogeneous catalysis (Costa et al., 2022; da Costa et al., 2022). Porous materials-based catalysts including biochar are relevant systems used in various processes due to their low cost and wide availability. They also facilitate the impregnation of substances that would otherwise be homogeneous in free form (Ma et al., 2013) The utilization of biochar in heterogeneous catalysis reduces the requirement for expensive commercial catalysts (Lokman et al., 2016; Tamborini et al., 2019).

Various examples of biochar-based catalysts employed in esterification reactions (Araujo et al., 2019; Corrêa et al., 2020) and transesterification reactions (Bastos et al., 2020; Mares et al., 2020) are available in literature. Thus, there are feasible alternatives to agro-industrial biomass residues, such as açaí seeds (Araujo et al., 2019; Mares et al., 2020), cupuaçu seeds (Mendonça et al., 2019), murumuru seed husk (Bastos et al., 2020; Corrêa et al., 2020), passion fruit peel (Almeida et al., 2021), sugarcane bagasse (Nazir et al., 2021), cocoa shell (Mendaros et al., 2020), palm residue (Alhothali et al., 2021), and orange skin (Lathiya et al., 2018). These reports demonstrate the viability of utilizing alternative biomass for catalyst synthesis, addressing both technical and economic considerations and offering successful case studies in various applications. Among the alternative biomasses mentioned, Brazil nut emerges as a relevant residual biomass with catalytic potential. It represents a non-timber forest product that is abundantly distributed in the Amazon rainforest (Souza et al., 2021). The Brazil nut tree (*Bertholletia excelsa* H.B.K.) yields seeds recognized as Brazil nuts and stands as one of the largest trees within the Amazon rainforest (refer to Fig. 1). Legal protection, such as Law 4771, prohibits the logging of this tree. The Brazil nut fruit, often referred to as the hedgehog (see Fig. 1A), comprises approximately 20 triangular-shaped seeds enveloped by a woody shell (integument), with the edible almond inside. In conventional commercial extraction processes, approximately 90% of waste is typically generated (Andrade et al., 2017).

The Brazil nut industry stands as one of the primary economic activities in the Amazon region, supporting several businesses and significantly contributes to the livelihoods of numerous individuals owing to the high value associated with this industry (Melo et al., 2015). Brazil produced 32,900 tons of Brazil nuts in 2019 (“IBGE”, 2019). Processing one ton of Brazil nut kernels generates 1.4 tons (70–90%) of waste, which is typically disposed of in an inappropriate manner (Dos Anjos et al., 2017; Nogueira et al., 2014).

The use of Brazil nut residues to produce biochar is of utmost importance as this product can add value to a significant proportion of the material that is inappropriately disposed of in the envi-

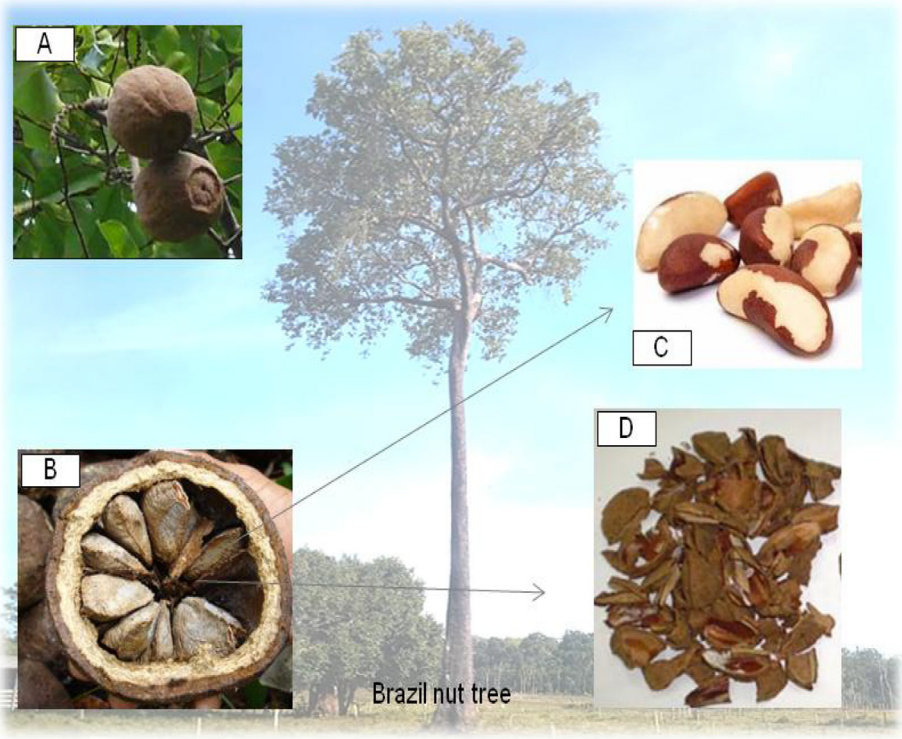

Fig. 1. Brazil nut tree, including the A) hedgehog, B) hedgehog with chestnuts, C) almond, and D) husks.

ronment. There have been few studies reported on the reuse of these residues for the production of activated carbon (Melo et al., 2015; Souza et al., 2021). Among the limited studies conducted, none have addressed the oxidation of isoeugenol using biochar from Brazil nut byproducts. Therefore, we aim to expand the literature on the production of biochar using residual Brazil nut biomass. We modified the biomass with 12-tungstophosphoric acid (HPW) through sonication without acid treatment to obtain catalysts in a sustainable and economically viable way. We report the first synthesis of a highly active catalyst for the isoeugenol oxidation reaction and evaluate its reusability.

2. Experimental section

The Brazil nut shells (fresh and collected at the Ver-O-Peso market) were washed with running water, then dried in an 80 °C oven for 8 h. Next, they were ground in a knife mill, passed through a 1 mm sieve, and calcined in a tubular furnace under the following conditions: 600 °C for 30 min, with a heating rate of 10 °C min^{-1} and a nitrogen flow rate of 50 mL min^{-1} (Ferreira and Foletto, 2016). To prepare the catalyst, 1 g of biochar was added to a beaker and 50 mL of distilled water was added. The beaker was placed in an ultrasonic bath for 2 h. Next, 0.56 g of 12-phosphotungstic acid (Sigma-Aldrich), which was equivalent to 30% by mass of tungsten, was added (Yu et al., 2018), and the contents were stirred for 1 h. The solution was dried in an oven at 110 °C for 12 h and calcined in a muffle furnace at 200 °C for 2 h. The resulting sample was labeled as 30HPW/CC(200–2).

Isoeugenol (0.8 mL) was mixed with H_2O_2 (ratio 1:10) and acetonitrile (ratio 1:32) in a round-bottom flask. 6% of the catalyst was subsequently added to the mixture. The system was continuously stirred and heated to 80 °C for 60 min. After the reaction, the catalyst was recovered by centrifugation and washed three times with acetonitrile to remove any residues (Franco et al., 2017a).

3. Results and discussion

3.1. Characterization of the catalyst 30HPW/CC(200–2)

The FTIR spectrum of the biochar is depicted in Fig. 2, displaying functional groups associated with the three components of the biomass. The band within the 3200 to 2750 cm^{-1} range corresponds to aliphatic C—H stretching, while stretching vibrations within the 1600 to 1800 cm^{-1} range are attributed to C=C vibrations in aromatics and olefins, with the C=C vibrations being centered around 1750 cm^{-1}. The set of bands extending from 1000 to 1500 cm^{-1} is related to C—OH stretches and flexion modes of alcoholic, phenolic, and carboxylic groups. Bands within the 800 to 500 cm^{-1} range correspond to out-of-plane aromatic C—H vibrations, as reported in the literature. (Apaydin-Varol and Pütün, 2012). In addition, the symmetrical stretching band of the C—O group, which is present in cellulose, hemicellulose, and lignin, appears at approximately 1250 cm^{-1}.

The Keggin anion, $PW_{12}O_{40}^{3-}$, present on the surface of the biochar serves as a model for this type of heteropoly acid. This anion is composed of a PO_4 tetrahedron surrounded by four W_3O_{13} groups made up of octahedra, as previously described in the literature. (Almeida et al., 2021; Caliman et al., 2005). The FTIR analysis of the catalyst (Fig. 2) was conducted to confirm the presence of tungsten on the biochar surface. The spectrum shows four oxygen bands for this compound, ranging from 700 to 1200 cm^{-1}. The characteristic bands for PO (1080 cm^{-1}), W=O (983 cm^{-1}), W—O and C—W (898 cm^{-1}), and W—O—W (797 cm^{-1}) are observed in the spectrum, confirming the presence of tungsten on the biochar surface (Almeida et al., 2021).

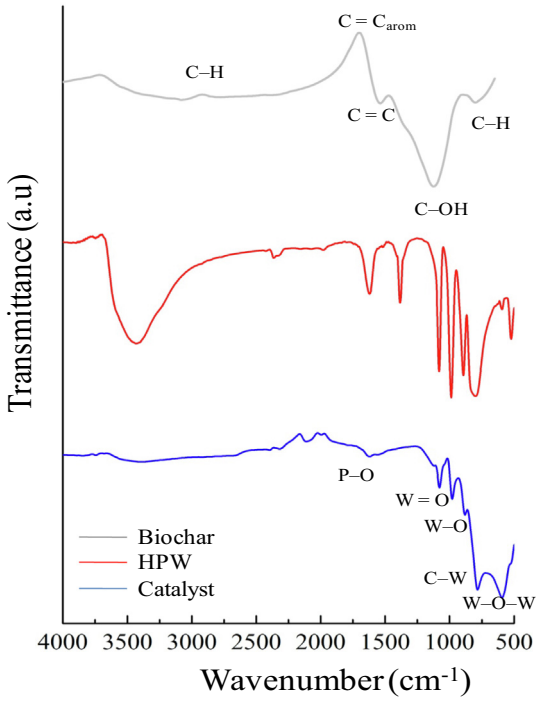

Fig. 2. FTIR spectra of the biochar, HPW, and catalyst.

X-ray diffraction (XRD) patterns of the biochar produced from Brazil nut bark (Fig. 3) show a typical pattern of amorphous carbonaceous material, with no peaks related to crystalline phases due to the thermal treatment at 600 °C. This result confirms that the material can serve as a catalyst support without requiring any chemical treatment.

The XRD pattern (Fig. 3) also shows that the material impregnated with HPW (catalyst) generated reflections characteristic of the WO_3 phase as the most abundant phase, followed by Ca $(WO)_4$, and a third phase containing phosphorus and tungsten (Almeida et al., 2021). The characteristic HPW peaks appear at 2θ = 10.3°, 25.3°, and 34.6°, which are consistent with the peak positions in the XRD pattern of the catalyst sample analyzed in this work. The intense characteristic peaks of HPW in the range of $10° \leq 2\theta \leq 50°$ in the pattern of the biochar supporting 30% HPW content confirm the effective impregnation, which is also supported by the energy-dispersive X-ray spectroscopy (EDS) analysis results shown in Fig. 4. These findings were in good agrément with previous reports (Almeida et al., 2021).

The production of carbon material from waste, coupled with subsequent surface modification, could represent a promising and appealing new application. The quantity and type of surface acidic sites i.e. tungsten are crucial factors influencing the suitability of such carbon materials (Goncalves et al., 2015). Fig. 3 illustrates the incorporation of HPW in the biochar, and the total elemental content was characterized using EDS (Figs. 4 and 5) and UV–Vis spectrophotometry (Fig. 6).

3.2. Energy dispersive X-ray spectroscopy (EDS)

The chemical composition of the materials was determined via EDS analysis. The results indicated a higher carbon content in both the biochar (Fig. 4) and the catalyst (Fig. 5), which can be attributed to the pyrolysis process (Bastos et al., 2020; Corrêa et al., 2020). The analysis of the biochar shows that more than 82% of the carbon content is from the pyrolysis process (Fig. 4), which is expected. However, the 30HPW/CC(200–2) sample (referring to 30% HPW,

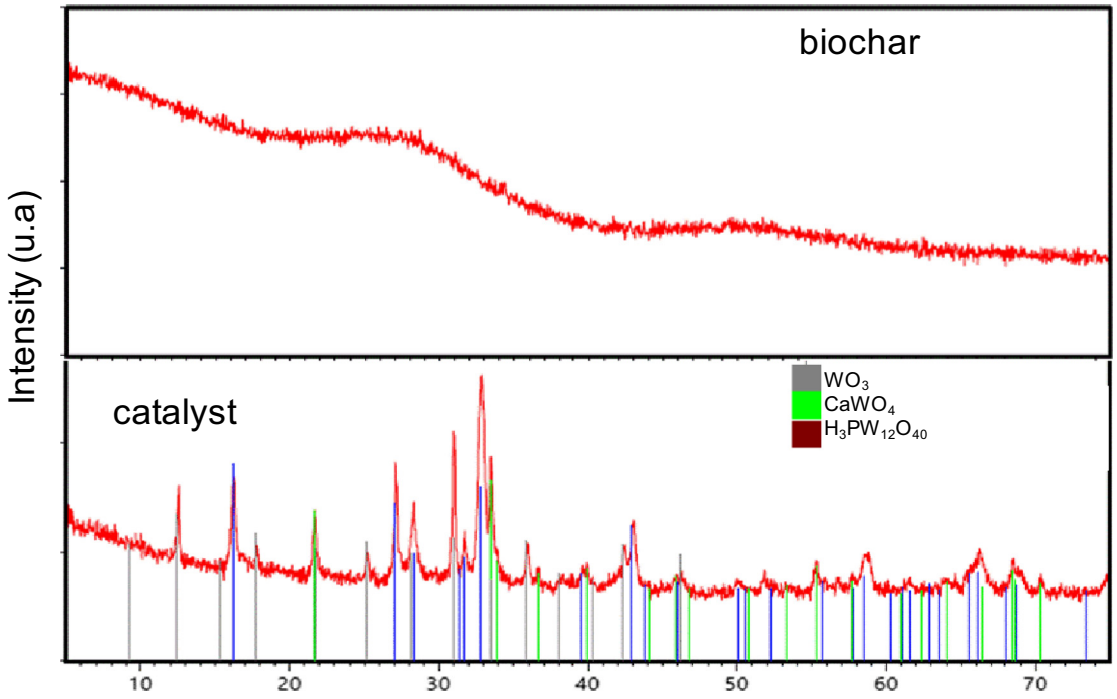

Fig. 3. XRD patterns of the biochar and catalyst.

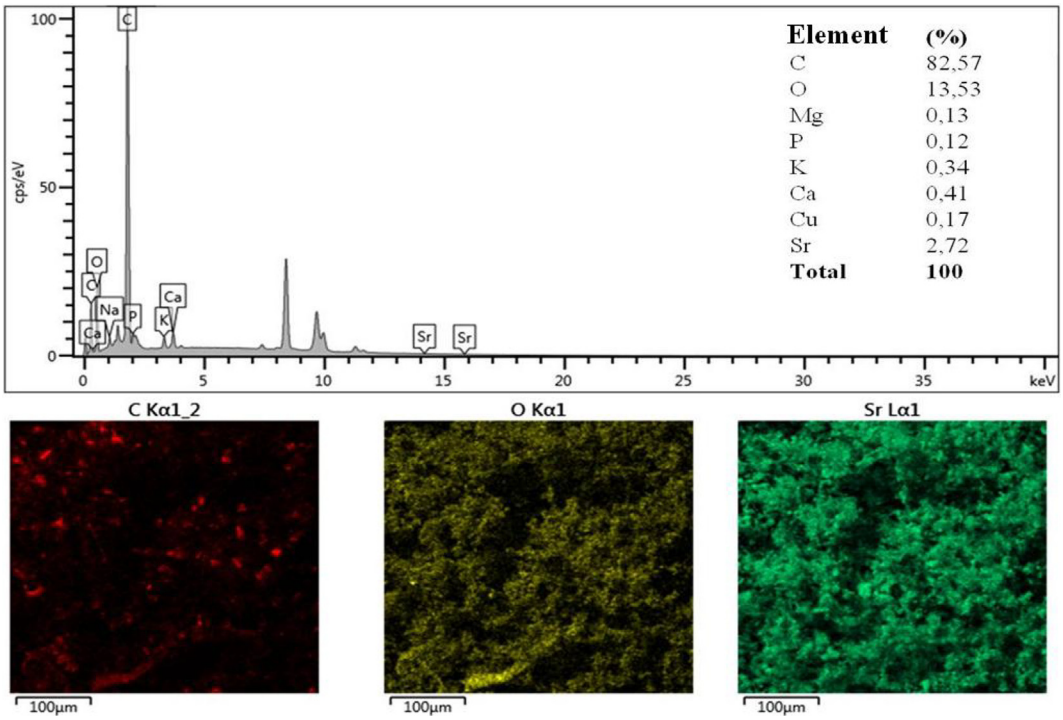

Fig. 4. Biochar EDS analysis results.

chestnut charcoal, 200 °C calcination, and 2-hour ultrasonic bath) has a tungsten content of 28.63% after impregnation (Fig. 5), demonstrating efficient incorporation of tungsten species in the biochar. The increase in oxygen content of the biochar after impregnation (from 13.53% to 16.60%) is another indication of HPW ($H_3PW_{12}O_{40}$) incorporation into the biochar's structure (Almeida et al., 2021). The analyses detected not only carbon but also other elements, including Na, K, Mg, Ca, P, Cu, and Sr, although carbon was the most abundant element. The dispersion of all elements was excellent with no clusters observed, as demonstrated by EDS analysis (Figs. 10 and 11). The actual tungsten content in this catalyst was found to be 28.63% by mass, which is close to the theoretical value of 30% relative to the mass of biochar. This similarity strongly indicates that the preparation and calcination conditions did not affect the adsorption of HPW onto the surface of the biochar. Although the actual loading amount of HPW

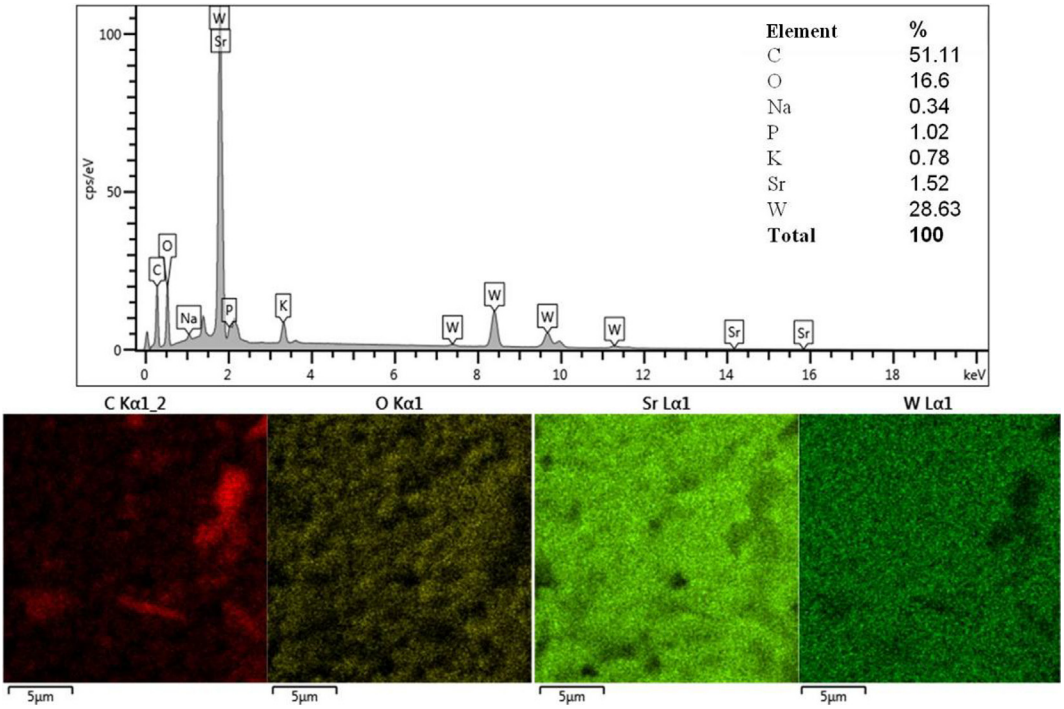

Fig. 5. Catalyst EDS analysis.

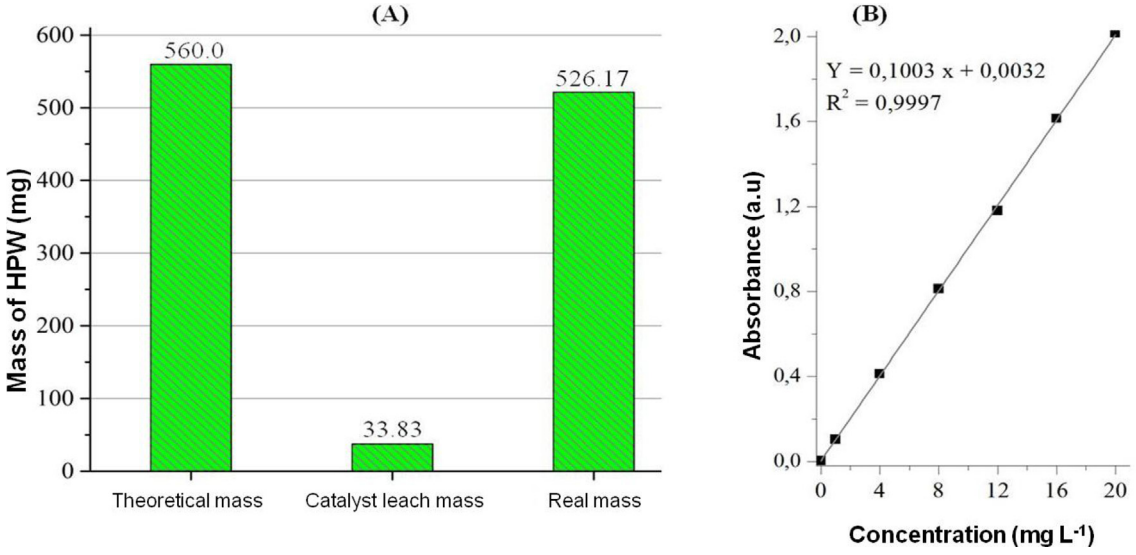

Fig. 6. A) Quantification of HPW loss using UV–Vis spectrophotometry, and B) the calibration curve used to determine the leaching of catalysts containing supported HPW.

(28.63%) is smaller than the theoretical amount, the solid is still referred to by its nominal composition.

UV–Vis spectrophotometric analysis of the ethanol-washed supernatant obtained from the modified sample (30HPW/CC (200–2)) provided information on the quantity of HPW that was not incorporated into the biochar (Fig. 6).

HPW content in matrices was determined by subtracting the amount of HPW measured in the supernatant using UV–vis spectrophotometry from the initial amount of HPW added (Oliveira et al., 2019b; Pezzotta et al., 2018). Based on results presented in Fig. 6, 30HPW/CC(200–2) experienced a partial loss of approximately 33.83 mg of HPW, indicating that 6% of the initially incorporated HPW was leached out. This finding is consistent with the EDS analysis results shown in Fig. 5.

EDS and UV–Vis results mentioned above confirm that not all of the HPW species in the initial synthesis solution were attached to the biochar structure. This has been observed in previous studies as well (Alsalme et al., 2008; Oliveira et al., 2019b; Pezzotta et al., 2018; Pires et al., 2014). As for the EDS analysis, the results are consistent with those of the FTIR and XRD analyses, confirming the incorporation of HPW into the biochar structure. The EDS mapping images of the biochar and catalyst are shown in Figs. 4 and 5, respectively.

3.3. Scanning electron microscopy (SEM)

SEM was employed to analyze the surface morphology of the Brazil nutshell biochar. SEM images (Fig. 7A and B) depict an

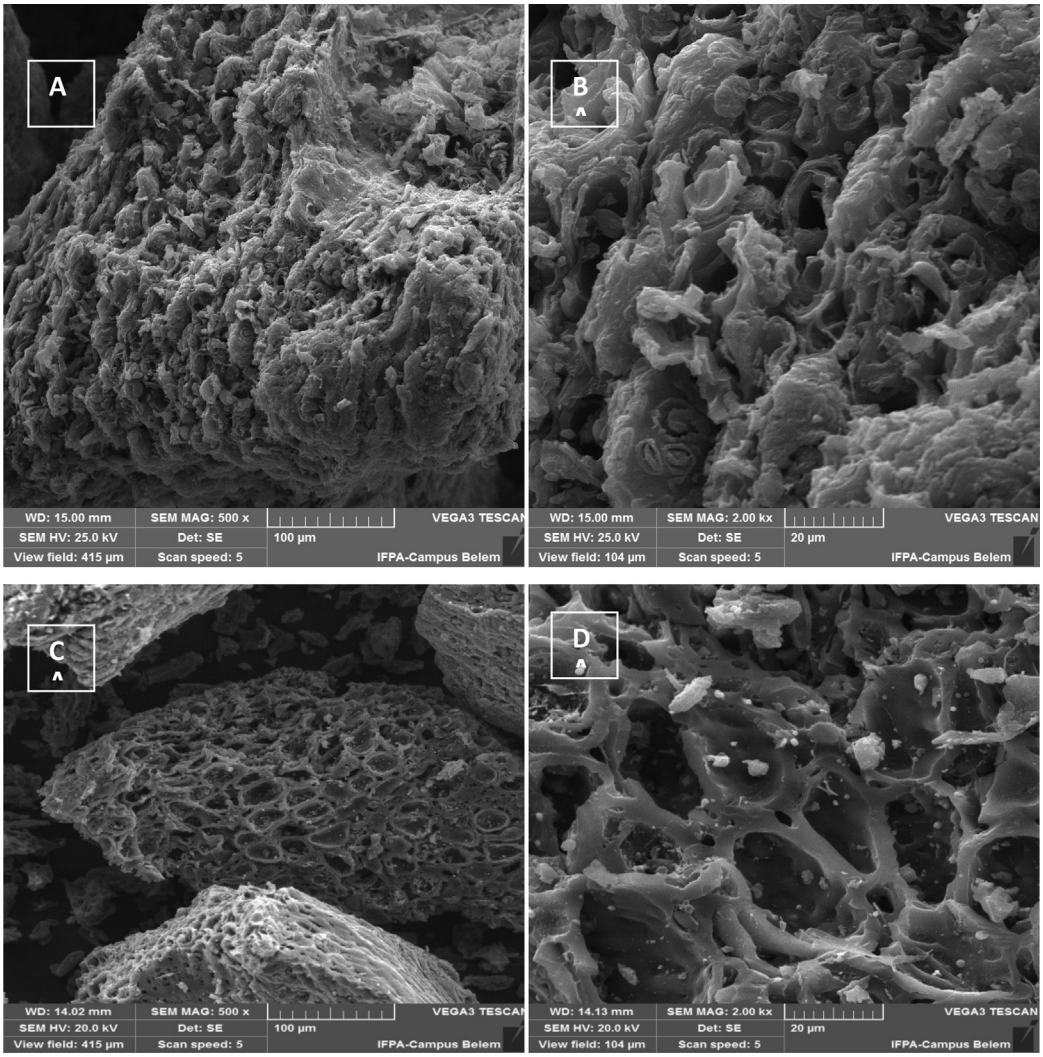

Fig. 7. SEM micrographs of the biochar at A) 500 × and B) 2000 × magnification and the catalyst at C) 500 × and D) 2000 × magnification.

irregular yet uniform surface structure characterized by pore cavities and a distinct porous pattern, a typical attribute of charred organic waste (Corrêa et al., 2020). During the pyrolysis process of lignocellulosic materials, volatile compounds are emitted and interact with the biomass, leading to surface melting and the creation of vesicles or bubbles (Conz et al., 2015). Fig. 7C and D illustrate the catalyst's images, showing a heterogeneous surface structure, along with an irregular surface morphology with a well-developed elongated pore structure (Linhares et al., 2016).

3.4. Catalytic tests of isoeugenol oxidation

The selective oxidation of isoeugenol to vanillin using hydrogen peroxide as oxidizing agent (Fig. 8) was employed as test reaction for the synthesized catalysts. Vanillin is produced from isoeugenol by oxidative cleavage of the C═C bond to C—C, followed by cleavage to the aldehyde (Franco et al., 2017a, 2019; García-Albar et al., 2021). The objective of these experiments was to evaluate the efficiency of the catalyst in the reaction to produce vanillin, as shown in Figure S7.

In order to evaluate the selective oxidation of isoeugenol to vanillin using hydrogen peroxide as an oxidizing agent, the reaction was monitored and analyzed by gas chromatography (GC) to quantify and identify the vanillin and other compounds produced during the reactions. Nevertheless, it is worth noting that the oxidative conditions involving peroxide employed in this study may inadvertently lead to the formation of undesired products through side reactions (García-Albar et al. 2021). GC analysis of the product mixtures identified four primary compounds: (a) vanillin, (b) vanillyl methyl ketone, (c) eugenol, and (d) methyl

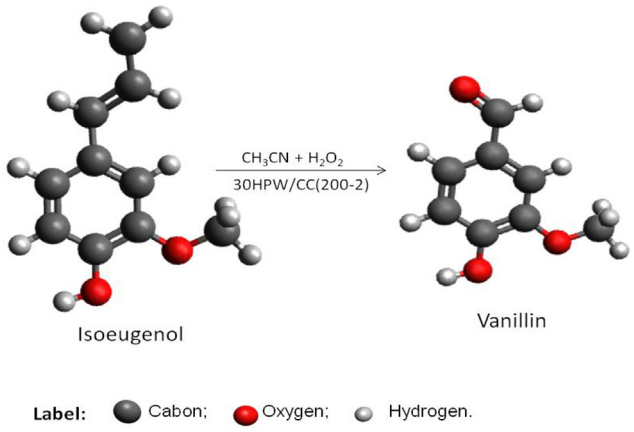

Fig. 8. Oxidation reaction of isoeugenol to vanillin.

3-hydroxy-4-methoxyphenylacetate, as illustrated in Fig. 9. The chromatographic profiles of the reactions were additionally assessed and depicted in Figures S1–S4.

Blank runs conducted in the absence of a catalyst demonstrated nearly negligible conversion (<10%). Surprisingly, a notable selectivity toward vanillyl methyl ketone (>54%) was observed (Fig. 10), highlighting the significance of this compound in the reaction mechanism, consistent with findings reported in previous studies (FILICIOTTO et al., 2021). The use of unmodified biochar exhibited a low conversion of isoeugenol (<16%) and low selectivity toward vanillin (<20%) and methyl 3-hydroxy-4-methoxyphenylacetate (<21%) compared to the selectivity toward vanillyl methyl ketone (28%) as the main products. Therefore, it can be inferred that the catalytic activity is mainly due to HPW. A control experiment was also conducted with HPW in an amount close to 27 mg (referring to the actual charge impregnated in the biochar used in each reaction), resulting in high conversion (>73%) of isoeugenol and high selectivity (>35%) toward vanillin (Fig. 10).

Both pure HPW and 30HPW/CC(200–2) achieved nearly complete conversion of the starting material. Although the selectivity of both catalysts was comparable in terms of starting-material conversion, the 30HPW/CC(200–2) catalyst demonstrated superior selectivity (<54%) (Fig. 10). This outcome could be attributed to a "trapping" effect of HPW and isoeugenol within the pores of 30HPW/CC(200–2), resulting in reduced levels of side products, consistent with findings reported in prior studies (Franco et al., 2017; García-Albar et al. 2021; Marquez-medina et al., 2018). Consequently, the utilization of either pure HPW or 30HPW/CC(200–2) led to substantial conversions within the system, underscoring the role of HPW as the active catalytic phase.

The results obtained in this study after a 60-minute reaction closely resemble those reported by Franco et al. Franco et al. (2017), who used a Nb/Al-SBA-15 catalyst in the oxidation of isoeugenol under optimized conditions (69% conversion, 66% vanillin selectivity in 2 h of reaction at 90 °C). Bohre et al. (Bohre et al., 2017) demonstrated that the CuO_x(20)/rGO catalyst supported on reduced graphene oxide is efficient in oxidizing isoeugenol with high conversion (87%) and vanillin yield (53%) under mild reaction conditions (50 °C). However, to reduce the formation of byproducts, the system needed to operate under 4 bar O_2 for 24 h.

3.5. Mechanism

Previous studies reported that the oxidation of isoeugenol to vanillin in similar systems proceeds with the participation of

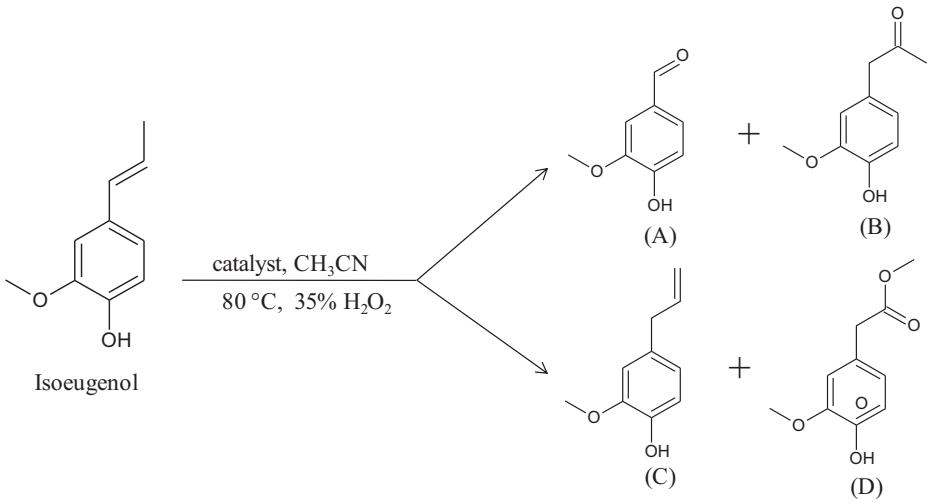

Fig. 9. Main oxidation products of isoeugenol: (A) vanillin, (B) vanillyl methyl ketone,(C) eugenol, and (D) methyl(3-hydroxy-4-methoxyphenyl).

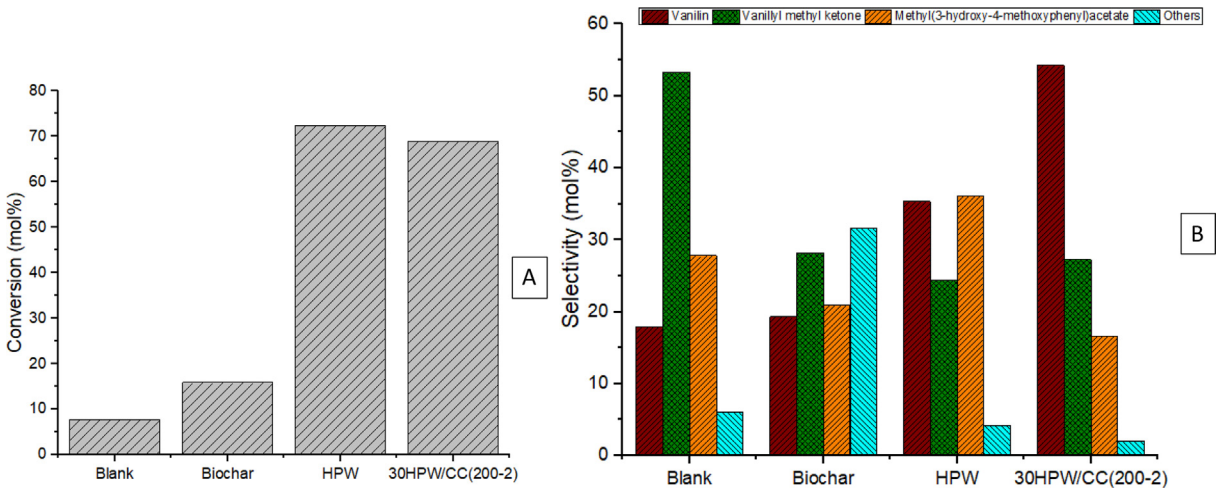

Fig. 10. A: Isoeugenol conversion values for blank and catalyst-assisted reactions; B: Product selectivity. Reaction conditions: 0.8 mL isoeugenol, 1.2 mL H_2O_2, 7 mL acetonitrile, 0.05 g catalyst, 80 °C, 1-hour reaction time. All reactions were conducted in triplicate to minimize potential errors.

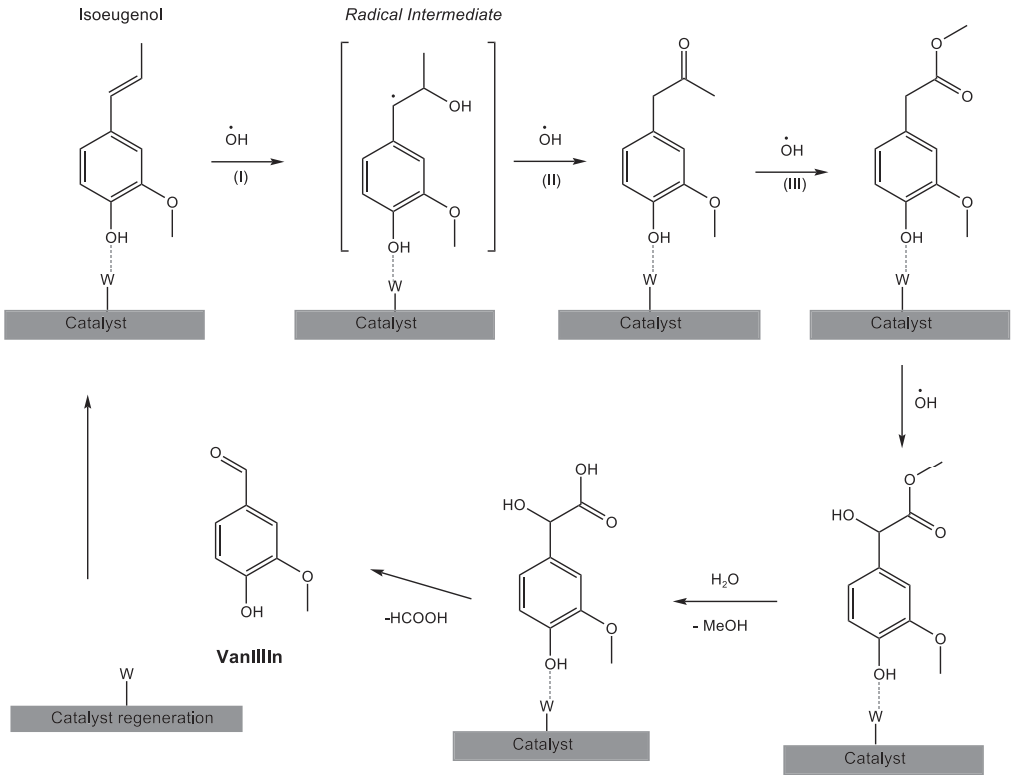

Scheme 1. Proposed radical mechanism of the conversion of isoeugenol to vanillin. (). Adapted from Filiciotto et al., 2021

hydroxyl radicals. (Filiciotto et al., 2021; Gusevskaya et al., 2012). Transition metals can generally catalyze via oxometal, decomposing hydrogen peroxide (H_2O_2) hydroxyl radicals (at the same time increasing the oxidation state of the metal), which then coordinates with the reactive molecule (substrate) (Filiciotto et al., 2021). In this sense, the oxygenation of isoeugenol into vanillin also proceeds with the participation of hydroxyl radicals, making the reaction efficient under the action of W on the biochar surface. With the substrate (isoeugenol) adsorbed on the active sites on the surface of the catalyst, it is attacked by the hydroxyl radical (I) (Scheme 1). The step of interaction between hydroxyl radicals and isoeugenol leads to the formation of the intermediate radical that readily reacts with hydroxyl radical and forms vanillyl methyl ketone (II) which reacts with another hydroxyl radical to form methyl(3-hydroxy-4-methoxyphenyl (III). If this latter product (III) is an intermediate of vanillin synthesis, it could undergo a series of steps involving unconcerted hydrogen radical abstraction, hydroxylation, ester hydrolysis, and cleavage to form vanillin and formic acid (Filiciotto et al., 2021), eventually cleaving the bond of vanillin and regenerating the acidic site in the catalyst.

3.6. Catalyst reusability

Investigating the reuse of heterogeneous catalysts is crucial as it allows for cost reduction and process optimization. The use of heterogeneous catalysts offers the benefit of producing the desired product through a clean process without requiring complex purification treatments. Furthermore, the catalyst can be recovered and reused without significant loss of catalytic activity, which is advantageous from both economic and environmental perspectives (Akinfalabi et al., 2017). 30HPW/CC(200–2) was reused in the oxidation of isoeugenol to evaluate its reusability. Four consecutive reactions were conducted using the same catalyst. After each cycle, the catalyst was recovered by centrifugation, washed with acetonitrile and dried at 120 °C (Franco et al., 2017b).

Isoeugenol conversion rate and vanillin selectivity gradually decreased after the first run, with catalytic activity significantly reduced after the third use (Fig. 11A and B). However, 30HPW/CC (200–2) demonstrated a maximum isoeugenol conversion rate of 69% with excellent vanillin selectivity of 55% under optimal conditions, and its recyclability was comparable to that of other heterogeneous catalysts. The improved activity observed during recycling studies could be attributed to the presence of tungsten as an oxo-species (WO^3), formed in the presence of peroxide.

All results and trends, both in terms of conversion and selectivity, were verified by both UV–Vis and GC analyses, with similar numerical values observed between the two techniques.

The results obtained in this study are in good agreement with a previous report (Ashengroph, 2017) that employed both GC–MS and UV–Vis analyses to evaluate the oxidation of eugenol (an isomer of isoeugenol). The numerical values obtained from both techniques were also comparable.

Deactivation due to leaching is a common phenomenon in this type of catalytic system. Measurable amounts of HPW were detected in the supernatant solution after the reaction, as analyzed by UV–Vis. Additionally, changes in the HPW content in the reused catalyst (as measured by UV–Vis) were observed in several subsequent measurements. These results are presented in Figures S5-A and S5-B.

UV–Vis analysis showed that the recovered catalyst used in each cycle had a slight decrease in HPW content from 26.31 mg. g^{-1} in the fresh 30HPW/CC(200–2) catalyst to 25.18 mg.g^{-1} in the recovered material (Figure S5-A). The average amount of leached HPW found in the analyzed samples for 30HPW/CC(200–2) after the first use was <1% of the initial amount loaded in the fresh catalyst, which might also explain the observed decrease in cat-

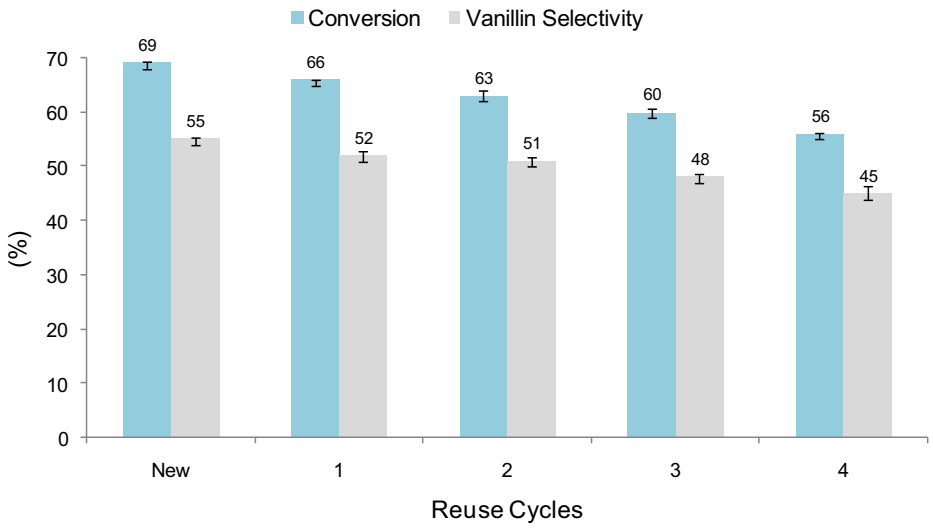

Fig. 11. Comparison of the catalytic activity in terms of conversion and vanillin selectivity of 30HPW/CC(200–2) catalyst for isoeugenol oxidation, as evaluated by UV–Vis (gray) and GC–MS (blue) analyses. Reaction conditions:0.8 mL of isoeugenol, 1.2 mL of H_2O_2, 7 mL of acetonitrile, 0.05 g of catalyst, 80 °C, 1 h of reaction.

alytic activity after the first reuse (Figure S5-B). However, the 30HPW/CC(200–2) catalyst exhibited good catalytic performance during the four reuse cycles, which correlates well with the low HPW content in the solution (<2% of the initial amount in the catalyst) after each reuse, as determined by UV–Vis. These results suggest that the amount of HPW leached from the biochar support was within acceptable limits (3%), as reported in previous studies (Almeida et al., 2021; Oliveira et al., 2019b).

Despite the observed decrease in catalytic activity and selectivity, the consistency of both parameters during the repeated use of the catalyst suggests that it remained active throughout the recycling process. This consistency may be attributed to the leaching of active HPW components during the washing and drying steps of the catalyst, as no additional HPW was added during reuse. In addition, mechanical damage caused by agitation during the reaction may have led to the leaching of WO_3, resulting in catalyst deactivation over subsequent reuses (Oliveira et al., 2019b; Pires et al., 2014) (Figure S5). However, the consistent activity of the catalyst in terms of vanillin yield during recycling implies that the leaching of a small amount of HPW species, possibly in the inactive form, does not significantly affect the activity of the homogeneous phase (Almeida et al., 2021).

3.7. Characterization of the reused catalyst

To ascertain the stability of the catalyst after multiple oxidation reactions of isoeugenol, a thorough catalyst characterization was conducted using FTIR, SEM and EDS analyses on the catalyst after the reuse cycles (see Figures S6-S9). These characterizations aimed to clarify the potential causes of catalyst deactivation during the reaction cycle.

Figure S6 depicts the FTIR spectrum of the catalyst after four reuse cycles. Notably, the spectrum still shows bands with vibrations characteristic of HPW even after being used in catalytic reactions. The main absorption bands for HPW were observed in the range of 700–1200 cm^{-1}, including typical bands for PO (1080 cm^{-1}), W═O (983 cm^{-1}), W—O and C—W (898 cm^{-1}), and W—O—W (797 cm^{-1} and 967 cm^{-1}). The spectrum suggests that the immobilized support retained its Keggin structure (HPW) even after being subjected to catalytic reaction conditions (Almeida et al., 2021).

Deactivation caused by carbonaceous deposits may be responsible for the observed decrease in activity, but no significant differences attributable to poisoning effects were observed in the FTIR spectra of the catalyst after the reaction. However, evidence of additional carbonaceous species deposited on the material was found in the EDS experiments (Figure S9).

SEM analysis (Figure S7) shows that the catalyst pores were obstructed after four reuse cycles (S7-B) compared to the new catalyst (S7-A). This obstruction may be due to the adsorption and/or deposition of compounds onto the support or catalyst degradation.

EDS analysis (Figures S8–S9) showed certain leaching from the catalyst at the end of the four reuse cycles, consistent with UV–Vis analysis results (Figure S5). The amount of tungsten in the catalyst decreased from 28.63% to 25.26% after four reaction cycles, but the amount of tungsten in the active phase remained high. 30HPW/CC (200–2) could be used for additional cycles of the isoeugenol oxidation reaction to efficiently produce vanillin. Conversion results (Fig. 11) indicated that the catalyst remained efficient after four reaction cycles, with a conversion rate and selectivity toward vanillin of over 50% and 40%, respectively.

FTIR, SEM, and UV–Vis techniques successfully confirmed the presence of active species in the material even after four reuses. Based on the findings of previous studies and results obtained in this study using 30HPW/CC(200–2), we anticipate that the proposed low-cost biochar can be used as a catalyst support in other organic transformation reactions, operating predominantly in a heterogeneous way.

3.8. Comparison of the catalytic conversion achieved using 30HPW/CC (200–2) with that achieved using other catalysts

To the best of our knowledge, this is the first report of using biochar derived from Brazil nut shells impregnated with HPW for the oxidation of isoeugenol to vanillin. The performance of this catalyst in the oxidation reaction exceeds that of previously reported catalysts, particularly in terms of cost-effectiveness (as shown in Table 1).

Table 1 shows that 30HPW/CC(200–2) and previously reported catalysts exhibit similar catalytic activities. For instance, the use of 1% Fe/RGO (1% iron ion and reduced graphene oxide support) led to a maximum vanillin yield of 63%, which is comparable to the yield

Table 1
Comparison of the catalytic performance of 30HPW/CC(200–2) catalyst with previously reported catalysts for selective oxidation of isoeugenol to vanillin.

Catalyst	Time (h)	Temperature (°C)	Conversion (%)	Selectivity (%)	Reuse cycles	Activity	Reference
(n-Bu)$_4$NVO$_3$ + pyrazine-2-carboxylic acid (PCA))[a]	2	80	71	50		–	(Gusevskaya et al., 2012)
Co-Hoba[b]	24		18	90	_	_	(Srinivasapriyan, 2020)
Ni-Hoba	24		23	92			
Cu-Hoba	24		10	82			
Cu-MINT[c]	6	80	69	66	3	30% (C) 57% (S)	(García-Albar et al. 2021)
1% Fe/RGO[d]	2	90	61	63			(Franco et al., 2017b)
0.5Fe/Al-SBA-15[e]	2	90	90	55	3	46% (S)	(Franco et al., 2017a)
0.5Nb/Al-SBA-15			69	66		39%(S)	
0.5Nb/Al-SBA-15			66	35		47%(S)	
CuO_x(20)/rGO[f]	24	50	97	53	4	52%(S)	(Bohre et al., 2017)
CoTPyP/TN[g]	24	50	87	72	3	71% (S)	(Adilina et al., 2012)
FeNMag-190[h]	24	25	85	57	5 at 90 °C	46% (S)	(Marquez-medina et al., 2018)
MCM-22 with cerium[i]	2	60	63	75	5	_	(Sahu et al., 2020)
30HPW/CC(200–2)	1	80	69	55	4	45%(S)	This work

(C) Conversion. (S) Selectivity.
[a] Vanadate anion salt n-Bu$_4$NVO$_3$ with H_2O_2 and pyrazine-2-carboxylic acid as a mediator; [b] Ultrathin ion nanosheets; [c] Supported metal nanoparticles on a silica matrix; [d] Iron ion and reduced graphene oxide support; [e] Mesoporous Al-SBA-15 with various ions; [f] Reduced graphene oxide supported copper oxide; [g] Taeniolite-intercalated Co–porphyrin using molecular oxygen as the sole oxidant; [h] Synthesis of iron oxide nanocatalysts; [i] Ce-containing MCM-22 zeolites with cerium.

obtained with the HPW-containing catalyst in the present study. Another example is the work of Gusevskaya et al. (Gusevskaya et al., 2012), who achieved lower vanillin yields (50%) under comparable conditions using a homogeneous and non-environmentally friendly catalyst in an amount approximately 50 times smaller (mol% of (n-Bu)$_4$NVO$_3$ + pyrazine-2-carboxylic acid (PCA)) than the amount of catalyst used in the present study. Marquez-Medina et al. (2018) obtained stable vanillin yields over three reuse experiments (90 °C). The spent FeMag-190 (iron oxide nanocatalysts) catalyst (after five reuses) was regenerated by calcination at 300 °C (in air, 2 h), recovering more than 80% of the initial catalytic activity of the fresh catalyst. Franco et al. (2017a) achieved a 69% conversion of isoeugenol to vanillin with a selectivity of 66% using SBA-15 aluminosilicates as a support for Nb. Meanwhile, when the researchers grouped various Fe-based materials together, they achieved a higher conversion of isoeugenol (90%) but a lower selectivity for vanillin (55%). The Cu-MINT material reported by García-Albar et al. (2021) demonstrated high catalytic activity, with 69% isoeugenol conversion and 66% vanillin selectivity during a 6-hour reaction. However, the material showed deactivation over three reaction cycles, resulting in reduced conversion and selectivity. The vanillin selectivity of 54% achieved with the low-cost carbon-based catalyst in this study is noteworthy when compared to previously reported values in Table 1. In conclusion, it is worth mentioning that the production costs of the catalyst derived from Brazil nut bark waste are promising. The utilization of this waste as an inexpensive raw material for producing catalytic supports has been proven feasible. Hence, the use of a byproduct from extractive production, such as chestnut shell, for synthesizing a novel catalytic material is sustainable and diminishes the environmental liability resulting from its disposal, while adding economic value to the waste.

4. Conclusions

30HPW/CC(200–2) exhibited high efficiency for four cycles of isoeugenol oxidation reactions. Characterization of the catalysts using EDS demonstrated a low leaching rate of the active phase. The catalyst showed a conversion rate and selectivity >40% and 50%, respectively, even higher than those of the autocatalysis reaction.

The best conditions for the oxidation reaction of isoeugenol to vanillin were carried out in this study at a temperature of 80 °C with a peroxide ratio of 1:10 in relation to isoeugen and 1:32 in relation to acetonitrile (as solvent), and a amount of 6% catalyst for 60 min. Under these conditions, a maximum isoeugenol conversion of 69% was achieved, with product distribution in the order of vanillin (>54%) > vanillylmethylketone (<28%) > methyl 3-hydroxy-4-methoxyphenylacetate (<18%). Pure HPW showed a conversion rate of 72% with a product distribution of methyl 3-hydroxy-4-methoxyphenylacetate (<37%) > vanillin (<36%) > vanillylmethylke tone (<25%).

The findings presented in this study could lead to the development of a more sustainable process for producing vanillin, a valuable food and perfume additive with high economic value. We anticipate that the results reported in this study will inspire further investigation into various applications of the 30HPW/CC (200–2) catalyst and biochar support, such as in oxidation reactions and heavy metal removal, among other potential applications.

Declaration of competing interest

The authors declare that they have no known competing financial interests or personal relationships that could have appeared to influence the work reported in this paper.

Acknowledgements

The authors express their gratitude to PROPESP/UFPA for their support. The work was also supported by CNPQ under grant number 315279/2021-4 and 313798/2022-2 (LASN grant), BASA 2022/233, and CAPES (AAFC doctoral grant and RJP master grant). This project was funded by the Researcher Supporting Project Number (RSP2023405), King Saud University, Riyadh, Saudi Arabia. This publication was supported by RUDN University Strategic Academic Leadership Program (R. Luque).

Appendix A. Supplementary material

Supplementary data to this article can be found online at https://doi.org/10.1016/j.arabjc.2023.105313.

References

Adilina, I.B. et al., 2012. Oxidative cleavage of isoeugenol to vanillin under molecular oxygen catalysed by cobalt porphyrin intercalated into lithium taeniolite clay. J. Mol. Catal. A Chem. 361–362, 72–79.

Akinfalabi, S.I. et al., 2017. Synthesis of biodiesel from palm fatty acid distillate using sulfonated palm seed cake catalyst. Renew. Energy 111, 611–619.

Alhothali, A. et al., 2021. Optimization of micro-pollutants' removal from wastewater using agricultural waste-derived sustainable adsorbent. Int. J. Environ. Res. Public Health 18 (21), 1–18.

Almeida, R.P. et al., 2021. Residue-based activated carbon from passion fruit seed as support to H3PW12O40 for the esterification of oleic acid. J. Cleaner Product. 282.

Alsalme, A., Kozhevnikova, E.F., Kozhevnikov, I.V., 2008. Heteropoly acids as catalysts for liquid-phase esterification and transesterification. Appl. Catal. A 349, 170–176.

Andrade, F., Magno, S., Mota, D.O., 2017. Produção de carvão ativado através de resíduos da Castanheira-do-Brasil (Bertholletia excelsa Bonpl.) voltados na solução para o tratamento de águas.

Apaydin-Varol, E., Pütün, A.E., 2012. Preparation and characterization of pyrolytic chars from different biomass samples. J. Analytical Appl. Pyrolysis 98, 29–36.

Araujo, R.O. et al., 2019. Low temperature sulfonation of acai stone biomass derived carbons as acid catalysts for esterification reactions. Energ. Conver. Manage. 196 (April), 821–830.

Ashengroph, M., 2017. Bioconversion of isoeugenol to vanillin and vanillic acid using the resting cells of Trichosporon asahii. **3**. Biotech 7 (6), 1–9.

Bastos, R.R.C. et al., 2020. Optimization of biodiesel production using sulfonated carbon-based catalyst from an amazon agro-industrial waste. Energy Conver. Manage. 205, (October 2019) 112457.

Bohre, A. et al., 2017. Aerobic oxidation of isoeugenol to vanillin with copper oxide doped reduced graphene oxide. ChemistrySelect 2 (10), 3129–3136.

Caliman, E. et al., 2005. Solvent effect on the preparation of H3PW12O40 supported on alumina. Catalys. Today 108, 816–825.

Conz, R.F., Abbruzzini, T.F., Pellegrino, C.E., 2015. Caracterização morfológica de biochars produzidos a partir de diferentes biomassas e temperaturas de pirólise. XXXV Congresso Brasileiro de Ciência do Solo 1, 1–5.

Costa, A.A.F.D. et al., 2022. Glycerol and catalysis by waste/low-cost materials—A review. Catalysts 12, (5) 570.

da Costa, A.A.F., de Oliveira Pires, L.H., Padron, D.R., Balu, A.M., da Rocha Filho, G.N., Luque, R. and do Nascimento, L.A.S., 2022. Recent advances on catalytic deoxygenation of residues for bio-oil production: an overview. 518.

da Luz Corrêa, A.P. et al., 2020. Preparation of sulfonated carbon-based catalysts from murumuru kernel shell and their performance in the esterification reaction. RSC Adv. 10 (34), 20245–20256.

de Nazaré de Oliveira, A. et al., 2021. An efficient catalyst prepared from residual kaolin for the esterification of distillate from the deodorization of palm oil. Catalysts 11, (5) 604.

de Oliveira, A.D.N. et al., 2019a. Bentonites modified with Phosphomolybdic Heteropolyacid (HPMo) for biowaste to biofuel production. Materials 12, (9) 1431.

de Oliveira, A.D.N. et al., 2019b. Acetylation of Eugenol over 12-Molybdophosphoric acid anchored in mesoporous silicate support synthesized from flint kaolin. Materials 12, (18) 2995.

Dos Anjos, D.B. et al., 2017. Potencial of Brazil chestnut bark as a biofertilizer on lactuca Sativa L. Culture. J. Chemical Information Model. 4 N1 (9), 193–199.

Ferreira, A.B., Foletto, E.L., 2016. Produção De Biochar a Partir De Pirólise De Biomassas E Sua Aplicação Como Adsorvente 9058–9069.

Filiciotto, I. et al., 2021. Continuous flow study of isoeugenol to vanillin: a bio-based iron oxide catalyst. Catal. Today 368 (November), 281–290.

Franco, A. et al., 2017a. selective oxidation of isoeugenol to vanillin over mechanochemically synthesized aluminosilicate supported transition metal catalysts. ChemistrySelect 2 (29), 9546–9551.

Franco, A. et al., 2017b. Mechanochemical synthesis of graphene oxide-supported transition metal catalysts for the oxidation of isoeugenol to vanillin. Beilstein J. Organic Chem. 13 (July), 1439–1445.

Franco, A. et al., 2019. Sewage sludge-derived materials as efficient catalysts for the selective production of vanillin from isoeugenol. ACS Sustain. Chem. Eng. 7 (8), 7519–7526.

Freitas, J.V., Nogueira, F.G.E., Farinas, C.S., 2019. Coconut shell activated carbon as an alternative adsorbent of inhibitors from lignocellulosic biomass pretreatment. Ind. Crop. Prod. 137 (May), 16–23.

García-albar, P. et al., rcía-Albar et al. 2021. Catalytic wet hydrogen peroxide oxidation of isoeugenol to vanillin using microwave-assisted synthesized metal loaded catalysts. Mol. Catal. 506 (March).

Goncalves, M. et al., 2015. Green acid catalyst obtained from industrial wastes for glycerol etherification. Fuel Process. Technol. 138, 695–703.

Gusevskaya, E.V. et al., 2012. Oxidation of isoeugenol to vanillin by the "H_2O_2-vanadate-pyrazine-2-carboxylic acid" reagent. J. Mol. Catal. A Chem. 363–364, 140–147.

IBGE.

Lathiya, D.R., Bhatt, D.V., Maheria, K.C., 2018. Synthesis of sulfonated carbon catalyst from waste orange peel for cost effective biodiesel production. Bioresource Technol. Rep. 2, 69–76.

Linhares, F.D.A., Marcílio, N.R., Melo, P.J., 2016. Estudo da produção de carvão ativado a partir do resíduo de casca da acácia negra com e sem ativação química Study of activated carbon production from the black wattle shell waste with and without chemical activation.

Lokman, I.M., Rashid, U., Taufiq-Ya, Y.H., 2016. Meso- and macroporous sulfonated starch solid acid catalyst for esterification of palm fatty acid distillate. Arab. J. Chem. 9 (2), 179–189.

Ma, C. et al., 2013. The high performance of tungsten carbides / porous bamboo charcoals supported Pt catalysts for methanol electrooxidation. J. Power Sources 242, 273–279.

Ma, Z., Dai, S., 2011.. Development of novel supported gold catalysts: a materials perspective. Nano Res. 4 (1), 3–32.

Mares, E.K.L. et al., 2020. Acai seed ash as a novel basic heterogeneous catalyst for biodiesel synthesis: optimization of the biodiesel production process. Fuel 299, (December 2020) 120887.

Marquez-medina, M.D. et al., 2018. Continuous-flow synthesis of supported magnetic iron oxide nanoparticles. ChemSusChem 11, 389–396.

Martău, G.A., Călinoiu, L.F., Vodnar, D.C., 2021. Bio-vanillin: towards a sustainable industrial production. Trends Food Sci. Technol.

Melo, S. et al., 2015. Production and characterization of absorbent heat from the bark of residual Brazil nut bark (Bertholletia Excelsa l.). Chem. Cent. J., 1–9

Mendaros, C.M. et al., 2020. Direct sulfonation of cacao shell to synthesize a solid acid catalyst for the esterification of oleic acid with methanol. Renew. Energy 152, 320–330.

Mendonça, I.M. et al., 2019. Application of calcined waste cupuaçu (Theobroma grandiflorum) seeds as a low-cost solid catalyst in soybean oil ethanolysis: Statistical optimization. Energ. Conver. Manage. 200, (September) 112095.

Nazir, M.H. et al., 2021. Waste sugarcane bagasse-derived nanocatalyst for microwave-assisted transesterification: Thermal, kinetic and optimization study. Biofuels Bioprod. Biorefin. 16, 122–141.

Nogueira, R. et al., 2014. Avaliação da carbonização do ouriço da castanha-do-brasil em forno tipo tambor. Sci. Electron. Arch. 6 (6), 7–17.

Pezzotta, C. et al., 2018. Improving the selectivity to 4-tert-butylresorcinol by adjusting the surface chemistry of heteropolyacid-based alkylation catalysts. J. Catal. 359, 198–211.

Pires, L.H.O. et al., 2014. Esterification of a waste produced from the palm oil industry over 12-tungstophosforic acid supported on kaolin waste and mesoporous materials. Appl. Catal. B. 160–161 (1), 122–128.

Queiroz, L.S. et al., 2020. Activated carbon obtained from amazonian biomass tailings (acai seed): modification, characterization, and use for removal of metal ions from water. J. Environ. Manage. 270, (January) 110868.

Rahman, A. et al., 2019. Chemical preparation of activated carbon from Acacia erioloba seed pods using H_2SO_4 as impregnating agent for water treatment: an environmentally benevolent approach. J. Clean. Prod. 237, 117689.

Reis, J.S. et al., 2019. Combustion properties of potential Amazon biomass waste for use as fuel. J. Therm. Anal. Calorim. 138 (5), 3535–3539.

Sahu, P., Ganesh, V., Sakthivel, A., 2020. Oxidation of a lignin-derived-model compound: Iso -eugenol to vanillin over cerium containing MCM-22. Catal. Commun. 145, (May) 106099.

Souza, C.D.R.D., Silva, K.D.C.D., 2021. Energy potential of waste from Brazil nut (Bertholletia excelsa H.B.K.) for production of activated carbon. Res. Soc. Dev. 10 (2), 1–13.

Spagnoli, A.A., Giannakoudakis, D.A., Bashkova, S., 2017. Adsorption of methylene blue on cashew nut shell based carbons activated with zinc chloride: The role of surface and structural parameters. J. Mol. Liq. 229, 465–471.

Srinivasapriyan, V., 2020. The surfactant-free bottom-up synthesis of ultrathin MOF nanosheets for the oxidation of isoeugenol to vanillin. Mater. Advan. 1 (3), 326–328.

Tamborini, L.H. et al., 2019. Application of sulfonated nanoporous carbons as acid catalysts for Fischer esterification reactions. Arab. J. Chem. 12 (8), 3172–3182.

Yu, H. et al., 2018. Microwave-assisted preparation of coal-based heterogeneous acid catalyst and its catalytic performance in esterification. J. Clean. Prod. 183, 67–76.